Nucleon matrix elements with $N_f = 2+1+1$ maximally twisted fermions

Simon Dinter[*][a], **Constantia Alexandrou**[b,c], **Martha Constantinou**[b], **Vincent Drach**[a], **Karl Jansen**[a] and **Dru Renner**[a][†]

[a]*NIC, DESY Zeuthen, Platanenallee 6, D-15738 Zeuthen, Germany*

[b]*Department of Physics, University of Cyprus, P.O. Box 20537, 1678 Nicosia, Cyprus*

[c]*Computation-based Science and Technology Research Center, The Cyprus Institute, 15 Kypranoros Str., 1645 Nicosia, Cyprus*

E-mail: simon.dinter@desy.de

We present the first lattice calculation of nucleon matrix elements using four dynamical flavors. We use the $N_f = 2+1+1$ maximally twisted mass formulation. The renormalization is performed non-perturbatively in the RI$'$-MOM scheme and results are given for the vector and axial vector operators with up to one-derivative. Our calculation of the average momentum of the unpolarized non-singlet parton distribution is presented and compared to our previous results obtained from the $N_f = 2$ case.

---

[*]Speaker.

[†]Current address: Jefferson Lab.

1. Introduction

The European Twisted Mass Collaboration (ETMC) is generating gauge configurations with four dynamical flavors: two degenerate light quarks and a pair of strange and charm quarks with their masses approximately fixed to their physical values ($N_f = 2 + 1 + 1$). Several volumes and lattice spacings smaller than 0.1 fm are being produced [1, 2]. We present here first results using the $N_f = 2 + 1 + 1$ formulation to calculate observables probing nucleon structure. In particular we show results for the non-singlet moment of the nucleon's unpolarized parton distribution $\langle x \rangle_{u-d}$. This is the lowest non-trivial moment of the quark momentum distribution. There are no disconnected contributions, which are computationally very demanding, and hence $\langle x \rangle_{u-d}$ can be computed relatively easily with lattice QCD. Furthermore, $\langle x \rangle_{u-d}$ is also known accurately from global analyses of experimental measurements, thus it provides a good benchmark for lattice computations of nucleon structure. The successful determination of $\langle x \rangle_{u-d}$ will provide confidence in the applicability of lattice QCD to predict other quantities of interest that might not be so well accessible experimentally.

The operators necessary to calculate nucleon structure require a renormalization and matching to the continuum scheme used to analyse the experimental measurements. The renormalization is performed non-perturbatively in the RI'-MOM scheme and then matched perturbatively to the continuum $\overline{MS}$ scheme to compare to the phenomenological results for the moments of parton distribution functions. In particular, we discuss the non-perturbative determination of the renormalization factors of the vector and axial vector operators with zero and one derivative.

Parton distribution functions (PDFs) are defined in Minkowski space and therefore are not directly accessible to lattice calculations. However, the moments of PDFs can be related to local operators that can be calculated in Euclidean space with lattice methods. The first moment of the parton distribution function, $q(x, \mu^2)$, is given by

$$\langle x \rangle_{q,\mu^2} = \int_{-1}^{1} dx \, x \, q(x, \mu^2) = \int_{0}^{1} dx \, x \left\{ q(x, \mu^2) + \overline{q}(x, \mu^2) \right\}. \tag{1.1}$$

We consider the isovector combination $\langle x \rangle_{u-d}$ in order to eliminate disconnected contributions. It can be determined by evaluating the expectation value of the local operator $O^{\mu\nu}$ given by

$$\langle p, s | \underbrace{\overline{q} \gamma^{\{\mu} iD^{\nu\}} \tau^3 q}_{O^{\mu\nu}} | p, s \rangle \big|_{\mu^2} = 2 \langle x \rangle_{u-d,\mu^2} p^{\{\mu} p^{\nu\}}. \tag{1.2}$$

Here q denotes the quark doublet (u, d) and τ^3 is the Pauli matrix acting on the flavor indices.

2. Lattice techniques

We use the Wilson twisted mass fermion action, which has the advantage of leading to physical observables that are automatically $\mathcal{O}(a)$ improved [3]. Our $N_f = 2 + 1 + 1$ setup, where we include dynamical up, down, strange and charm quarks, maintains this automatic $\mathcal{O}(a)$ improvement. Thus no operator improvement is necessary for $O^{\mu\nu}$ and $\langle x \rangle_{u-d}$ is accurate to $\mathcal{O}(a^2)$, thus providing an advantage compared to the improved Wilson actions that would require additional calculations for the operator improvement. In Table 1 we show the details of the ensembles used so far in this work.

The pion masses range from 320 to 450 MeV. The volumes satisfy $m_\pi L > 4$ in order to keep finite size effects small. The lattice spacing for the coupling $\beta = 1.95$ has been estimated in the mesonic sector to be $a \sim 0.078$ fm. Further details are available in Ref. [1].

β	L/a	$a\mu$	am_π	$\langle x \rangle_{u-d}$	stat.
1.95	32	0.0075	0.18020(27)(3)	0.252(7)	412
1.95	32	0.0055	0.15518(21)(33)	0.240(8)	843
1.95	32	0.0035	0.12602(30)(30)	0.236(20)	243

Table 1: In the first column we give the bare coupling. The second column is the spatial extent of the lattice and the temporal length is always $T = 2L$. The bare quark mass in lattice units is given in the third column. The fourth column is the pion mass in lattice units with the statistical and systematic errors. The results of $\langle x \rangle_{u-d}$ from this work are given in the fifth column and the sixth lists the number of configurations used in the calculation.

For the lattice calculation of $\langle x \rangle$ we need the evaluation of the proton three-point correlation function given by

$$C_{3p}\left(t_{\text{sink}} - t_{\text{source}}, t_{\text{operator}}\right) = \text{Tr}\,\frac{1 + \gamma_4}{2} \sum_{\mathbf{x}_{\text{operator}}, \mathbf{x}_{\text{sink}}} \left\langle J_p(t_{\text{sink}}, \mathbf{x}_{\text{sink}}) O^{44}(x_{\text{operator}}) \bar{J}_p(x_{\text{source}}) \right\rangle, \quad (2.1)$$

where $\bar{J}_p$ (J_p) is an appropriate proton lattice creation (annihilation) operator. The corresponding 2-point function is given by an identical expression but with the omission of the operator insertion. A standard ratio of the three-point function to the two-point function gives the desired matrix element in the large Euclidean-time limit: $t_{\text{operator}} - t_{\text{source}} \to \infty$ and $t_{\text{sink}} - t_{\text{operator}} \to \infty$.
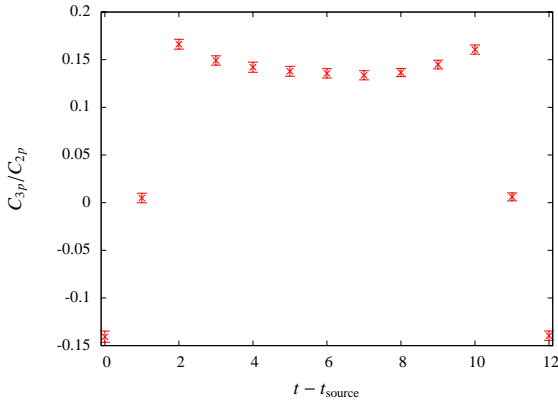

Figure 1: C_{3p}/C_{2p} as a function of $t_{\text{operator}} - t_{\text{source}}$ for fixed source-sink separation $t_{\text{sink}} - t_{\text{source}} = 12a$ on the ensemble with $m_\pi \approx 450$ MeV.

The ratio of C_{3p} and C_{2p} is computed as a function of t_{operator} and for large enough time separations it becomes a constant yielding the matrix element of interest. This is illustrated in Fig. 1, where we plot the dependence of the ratio on $t_{\text{operator}} - t_{\text{source}}$ for fixed source-sink separation $t_{\text{sink}} - t_{\text{source}} = 12a$. To evaluate C_{3p} we construct sequential propagators at the sink. In this approach one fixes the sink and source location, x and x'_4 respectively, as well as the quantum numbers of the initial and final states. The sum over the spatial $\mathbf{x}'$ can then be done implicitly by performing an inversion with a source constructed using the forward propagators generated at the source and the state at the sink.

The operator couples to the valence quarks at an intermediate time t_{operator}. Fixing the source-sink separation gives rise to contributions from excited states and, therefore, the source-sink separation has to be chosen sufficiently large to rule out those contributions but small enough to avoid the exponentially dropping signal-to-noise ratio. It is essential to use Gaussian smearing for the quarks in the proton interpolating fields J_p to increase the overlap of the creation and annihilation

operator with the ground state of the proton as well APE smearing for the gauge fields that enter the smearing functions to reduce noise. For the evaluation of the correlation functions we used the parallel contraction code ahmidas [4].

3. Results

In order to assess cut-off effects we examine the dependence on the lattice spacing, a, of the nucleon mass which has been computed at three different values of a. We show in Fig. 2 the nucleon mass as a function of $(a/r_0)^2$, where r_0 is the Sommer parameter. More details can be found in Ref. [5]. The observation is that the $\mathcal{O}(a^2)$ scaling is mild and compatible with zero. Additionally the dependence of $\langle x \rangle_{u-d}$ on the lattice spacing that we have found using the $N_f = 2$ ensembles [6, 7] is negligible. Therefore, we have reason to believe that the lattice cut-off effects for $\langle x \rangle_{u-d}$ using the $N_f = 2+1+1$ will also be small. We are currently investigating this issue.

Figure 2: The nucleon mass in units of r_0 as a function of $(a/r_0)^2$ for two reference pion masses.

The renormalization constants are computed non-perturbatively in the RI′-MOM scheme at different renormalization scales using the momentum source method [8]. The advantage of this method is a high statistical accuracy and the evaluation of the vertex for any operator including extended operators at no significant additional computational cost. For the details of the non-perturbative renormalization see Ref. [9].

In the RI scheme the renormalization constants are defined in the chiral limit. Since the mass of the strange and charm quarks are fixed to their physical values in these simulations, extrapolation to the chiral limit is not possible. Therefore, in order to compute the renormalization constants needed to obtain physical observations, ETMC has generated $N_f = 4$ ensembles at similar lattice spacings so that the chiral limit can be taken [10]. We present the renormalization factors for the local vector and axial vector operators Z_V^μ and Z_A^μ as well as for the one-derivative vector and axial vector operators, $Z_{DV}^{\mu\nu}$ and $Z_{DA}^{\mu\nu}$, respectively. The later fall into different irreducible representations of the hypercubic group, depending on the choice of the external indices, μ, ν. Hence, we distinguish between $Z_{DV1}(Z_{DA1}) = Z_{DV}^{\mu\mu}(Z_{DA}^{\mu\mu})$ and $Z_{DV2}(Z_{DA2}) = Z_{DV}^{\mu\neq\nu}(Z_{DA}^{\mu\neq\nu})$. Although we will use the $N_f = 4$ ensembles for the final determination of the renormalization constants it is interesting to compute the renormalization constants also in the $N_f = 2+1+1$ theory and study their quark mass dependence.

In Fig. 3 we show results for both the $N_f = 4$ and $N_f = 2+1+1$ ensembles in the RI′-MOM scheme. As can be seen, we obtain compatible values for all the operators. The same behavior is also observed in the case of Z_V and Z_A. This can be understood by examining the quark mass dependence of these results. In Fig. 4 we show, for the $N_f = 4$ case, the dependence of Z_V, Z_A, Z_{DV}, Z_{DA} on two light quark masses. The values we find are consistent with each other. This explains the
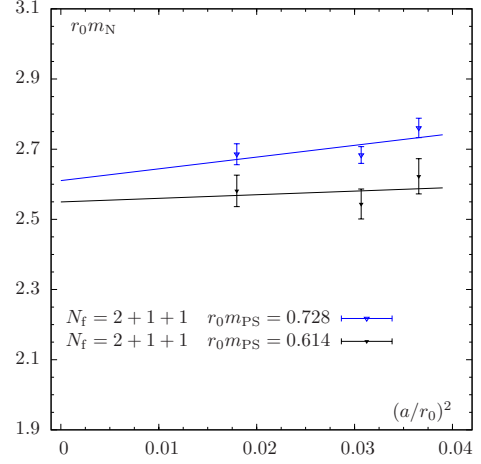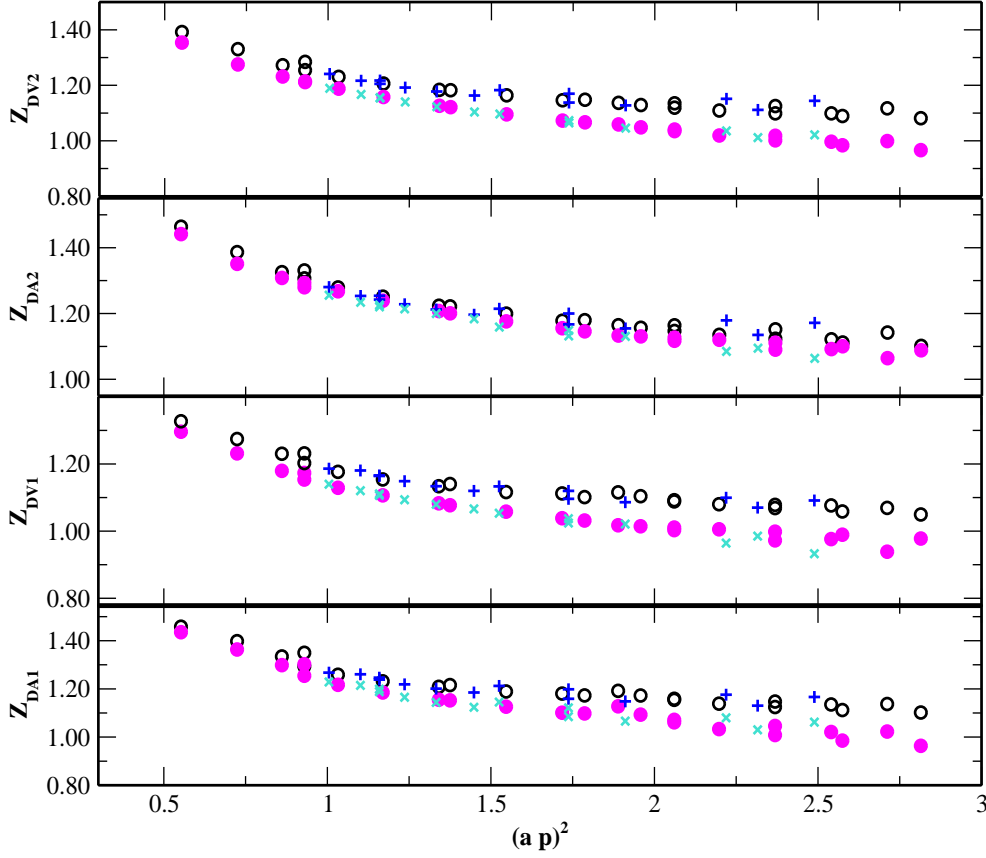
Figure 3: One-derivative renormalization constants as a function of the momentum squared in lattice units in the RI′-MOM scheme. We denote N_f=4 results by the open circles and N_f=2+1+1 by the crosses. Filled circles show the results after subtracting $\mathcal{O}(a^2)$ terms for the $N_f = 4$ case and x-symbols for the $N_f = 2 + 1 + 1$ case.

fact that the results in the $N_f = 4$ and $N = 2 + 1 + 1$ cases are compatible. Furthermore it makes any extrapolation of $N_F = 4$ results to the chiral limit straight forward.

The renormalization scale dependent Z_{DV} and Z_{DA} need to be converted to the continuum $\overline{\text{MS}}$-scheme, and for this we use a conversion factor computed in perturbation theory to $\mathcal{O}(g^6)$. They are also evolved perturbatively to a reference scale, which is chosen to be $(2 \text{ GeV})^2$. The constant that renormalizes $\langle x \rangle_{u-d}$ is Z_{DV1}. The results are shown in Fig. 5 both before subtracting the perturbative $\mathcal{O}(a^2)$-terms and after. Using the subtracted results, the preliminary value of Z_{DV1} in the $\overline{\text{MS}}$-scheme at $(2 \text{ GeV})^2$ is $Z_{DV1} = 0.998$ calculated using the $N_f = 4$ ensemble with $\beta = 1.95$ and $am_\pi = 0.194$.

In Fig. 6 we show the results for $\langle x \rangle_{u-d}$ for several pion masses for the $N_f = 2 + 1 + 1$ ensembles and give the values in Table 1. We compare with the $N_f = 2$ results for similar pion masses [11]. As can be seen, the $N_f = 2$ and $N_f = 2 + 1 + 1$ results are consistent showing that the effects of the strange and charm quarks in the sea are small compared to the, admittedly large, statistical errors. The results do not show a strong mass dependence and are higher than experiment. This behavior is consistent with the results of other collaborations [7, 12]. Thus calculations
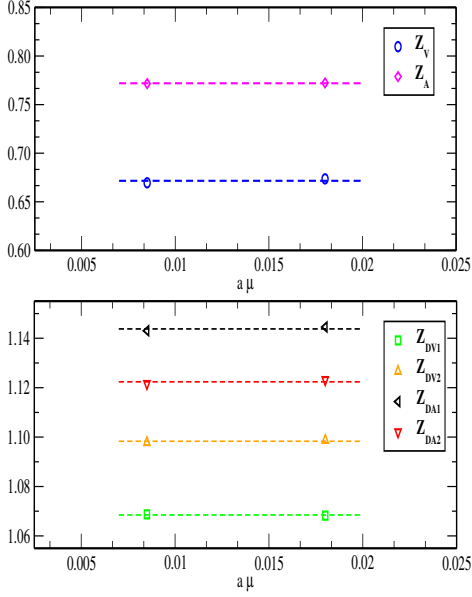
Figure 4: Z_V and Z_A (upper panel) and renormalization constants for the one-derivative operators (lower panel) as a function of the twisted mass. We have added 0.02 to the value of Z_{DA1} to distinguish it from Z_{DA2}.
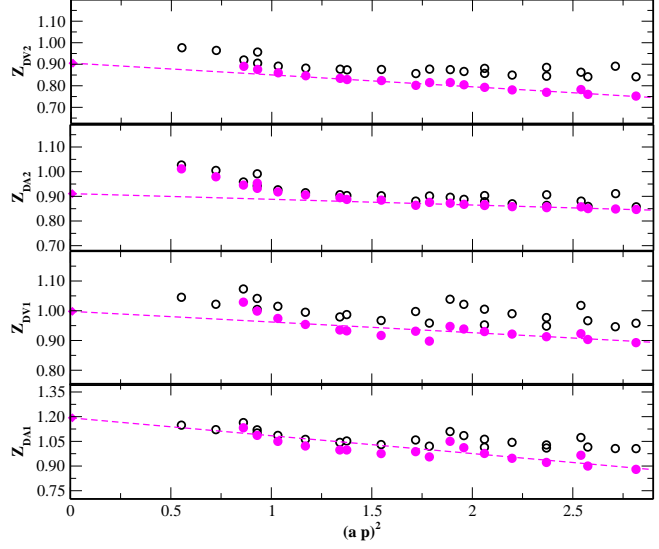
Figure 5: One-derivative renormalization constants as a function of the momentum squared in lattice units converted to the $\overline{MS}$-scheme for the $N_f = 4$ ensemble. Open circles denote results before perturbative subtraction of $\mathcal{O}(a^2)$-terms and filled circles denote the $\mathcal{O}(a^2)$-subtracted results.

at even lower pion masses are needed to shed light on the behaviour closer to the physical point.

4. Conclusions

We presented results on $\langle x \rangle_{u-d}$ with $N_f = 2 + 1 + 1$ twisted mass fermions for pion masses in the range of 320 MeV to 450 MeV at $\beta = 1.95$ ($a \sim 0.078\,\text{fm}$). We used non-perturbative renormalization calculated for an $N_f = 4$ ensemble at the same coupling. The results are in agreement with those obtained with $N_f = 2$ twisted mass fermions. As expected from $N_f = 2$, there is no strong mass dependence and the results are higher than experiment for the pion masses used in these calculations. The chiral behaviour of $\langle x \rangle_{u-d}$ will be studied using smaller pion masses and paying particular attention to excited state contributions in the three-point function.
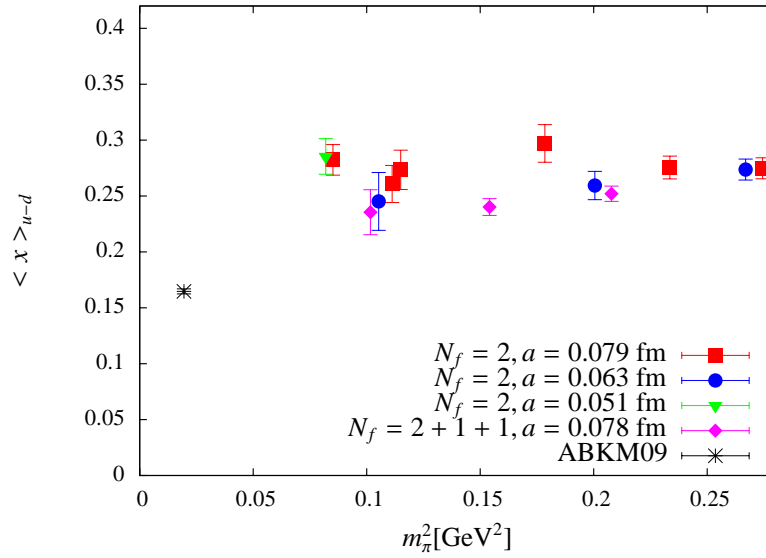
Acknowledgments

Figure 6: $\langle x \rangle_{u-d}$ obtained from $N_f = 2$ and from $N_f = 2+1+1$ ensembles for a range of pion masses. The experimental value was taken from the ABKM09 analysis [13].

References

[1] R. Baron *et al.*, JHEP **1006** (2010) 111 [arXiv:1004.5284 [hep-lat]].

[2] R. Baron *et al.*, PoS **Lattice 2009** (2009) 104 [arXiv:0911.5244 [hep-lat]].

[3] R. Frezzotti and G. C. Rossi, JHEP **0408** (2004) 007 [arXiv:hep-lat/0306014].

[4] A. Deuzeman, S. Dinter, S. Reker, Ahmidas – Parallelized contraction codes for lattice QCD
http://code.google.com/p/ahmidas

[5] V. Drach *et al.* [ETM Collaboration], PoS **Lattice 2010**, 101 (2010).

[6] C. Alexandrou *et al.* [ETM Collaboration], Phys. Rev. D **80** (2009) 114503 [arXiv:0910.2419 [hep-lat]].

[7] C. Alexandrou, Plenary talk at Lattice 2010, PoS **Lattice 2010**, 001 (2010).

[8] M. Göckeler, R. Horsley, H. Oelrich, H. Perlt, D. Petters, P.E.L. Rakow, A. Schafer, G. Schierholz, A. Schiller, Nucl. Phys. **B544** (1999) 699, [hep-lat/9807044].

[9] C. Alexandrou, M. Constantinou, T. Korzec, H. Panagopoulos, F. Stylianou, arXiv:1006.1920.

[10] D. Palao *et al.* [ETM Collaboration], Lattice 2010, in preparation.

[11] C. Alexandrou *et al.* [ETM Collaboration], in preparation.

[12] D. B. Renner, PoS **LAT2009**, 018 (2009), [arXiv:1002.0925 [hep-lat]].

[13] S. Alekhin, J. Blumlein, S. Klein, S. Moch, Phys. Rev. D81(2010) 014032, [arXiv:0908.2766 [hep-ph]].